Actin-binding protein 1 links B-cell antigen receptors to negative signaling pathways

Margaret K. Seeley-Fallen[a], Lisa J. Liu[a], Melanie R. Shapiro[a], Olusegun O. Onabajo[b], Senthilkumar Palaniyandi[c], Xiaoping Zhu[c], Tse-Hua Tan[d], Arpita Upadhyaya[e], and Wenxia Song[a,1]

[a]Department of Cell Biology and Molecular Genetics, University of Maryland, College Park, MD 20742; [b]Laboratory of Translational Genomics, National Cancer Institute, National Institutes of Health, Bethesda, MD 20892; [c]Laboratory of Immunology, Virginia–Maryland Regional College of Veterinary Medicine, University of Maryland, College Park, MD 20742; [d]Department of Pathology and Immunology, Baylor College of Medicine, Houston, TX 77030; and [e]Department of Physics, University of Maryland, College Park, MD 20742

Edited by Roberta Pelanda, National Jewish Health, Denver, CO, and accepted by the Editorial Board May 26, 2014 (received for review November 25, 2013)

Prolonged or uncontrolled B-cell receptor (BCR) signaling is associated with autoimmunity. We previously demonstrated a role for actin in BCR signal attenuation. This study reveals that actin-binding protein 1 (Abp1/HIP-55/SH3P7) is a negative regulator of BCR signaling and links actin to negative regulatory pathways of the BCR. In both *Abp1*$^{-/-}$ and bone marrow chimeric mice, in which only B cells lack Abp1 expression, the number of spontaneous germinal center and marginal zone B cells and the level of autoantibody are significantly increased. Serum levels of T-independent antibody responses and total antibody are elevated, whereas T-dependent antibody responses are markedly reduced and fail to undergo affinity maturation. Upon activation, surface BCR clustering is enhanced and B-cell contraction delayed in *Abp1*$^{-/-}$ B cells, concurrent with slow but persistent increases in F-actin at BCR signalosomes. Furthermore, BCR signaling is enhanced in *Abp1*$^{-/-}$ B cells compared with wild-type B cells, including Ca^{2+} flux and phosphorylation of B-cell linker protein, the mitogen-activated protein kinase kinase MEK1/2, and ERK, coinciding with reductions in recruitment of the inhibitory signaling molecules hematopoietic progenitor kinase 1 and SH2-containing inositol 5-phosphatase to BCR signalosomes. Our results indicate that Abp1 negatively regulates BCR signaling by coupling actin remodeling to B-cell contraction and activation of inhibitory signaling molecules, which contributes to the regulation of peripheral B-cell development and antibody responses.

B-lymphocytes | actin cytoskeleton | signal transduction

B cells are responsible for mounting antibody (Ab) responses towards invading pathogens. Antigen (Ag) binding to B-cell receptors (BCRs) induces rapid reorganization of surface BCRs into microclusters (1) and the interaction of the BCR with lipid raft-resident kinases, initiating signaling required for B-cell survival and proliferation (2, 3). BCR signaling is tightly regulated, and elevated or sustained BCR signaling has been shown to be associated with autoimmunity (4). Attenuation of BCR signaling is mediated by various phosphatases and kinases, including SH2-containing inositol 5-phosphatase (SHIP-1) (5) and hematopoietic progenitor kinase 1 (HPK1) (6). SHIP-1 inhibits activation of phospholipase-Cγ2 (PLCγ2), Bruton's tyrosine kinase, and Akt by eliminating their membrane docking sites, consequently blocking their downstream signaling (5). SHIP deficiency causes hyperresponsiveness and impaired affinity maturation of B cells in germinal centers (GCs) (7). HPK1 inhibits BCR signaling by inducing phosphorylation and subsequent ubiquitination of B-cell linker protein (BLNK) (6), the key adaptor molecule of the BCR. HPK1 deficiency results in elevated levels of activated BLNK, MAP kinases, B-cell proliferation, and resultant susceptibility to induced autoimmunity (6). BCR clustering is also involved in negative regulation, as we recently demonstrated that coalescence of BCR microclusters into a central cluster facilitates BCR signal attenuation. This coalescence requires actin-mediated B-cell contraction and SHIP-1 activation (8, 9).

Actin is critical for both amplification and attenuation of BCR signaling. BCR-induced disassembly of cortical actin enables BCR microcluster formation and signal activation (1, 10, 11). Actin reassembly expands the contact of B cells with Ag-presenting surfaces and induces polarized movement of surface BCRs, enhancing BCR clustering and signaling (8–10, 12, 13). Upon maximal cell spread, F-actin decreases in the B-cell region contacting Ag-presenting surfaces, and the cells contract, facilitating coalescence of BCR microclusters and signal attenuation (1, 8, 9, 13). Persistent actin accumulation at the B-cell contact zone and delayed cell contraction, caused by B-cell–specific neuronal Wiskott-Aldrich syndrome protein (*N*-WASP) knockout, lead to enhanced BCR signaling and elevated levels of autoantibody (autoAb) (14). These data indicate that actin remodeling coordinates with the reorganization and signaling of surface BCRs, but how actin attenuates BCR signaling remains elusive.

Abp1 is an adaptor protein that contains multiple interaction domains, including an actin-depolymerizing factor homology, helical, proline-rich, and SH3 domains (15–17). Its ability to simultaneously bind F-actin and proline-rich-domain-containing molecules implicates a role for Abp1 in actin–BCR communication. A role for Abp1 in lymphocyte signaling was first demonstrated in Abp1-deficient T cells, which display decreased signaling, proliferation, cytokine production, and T-cell-dependent Ab responses (18). Abp1 is responsible for recruiting HPK1 to the immunological synapse of T cells (19). In B cells, BCR activation induces the recruitment and phosphorylation of Abp1 (15, 20), which is required for BCR-mediated Ag

Significance

B cells are the major mediators of humoral immunity, producing antibody to aid in the elimination of pathogens. B cells signal through their membrane receptors, resulting in transcriptional modification for the maintenance of B-cell survival, proliferation, and antibody production. B-cell receptor (BCR) signaling is tightly regulated, and elevated or sustained BCR signals lead to loss of B-cell tolerance and subsequent autoimmunity. This study reveals that the adaptor molecule Abp1 negatively regulates development of marginal zone and spontaneous germinal center B cells, as well as autoantibody production. As a link between the actin cytoskeleton and BCR signaling, Abp1 assists BCR signal attenuation by promoting BCR central cluster formation, as well as recruitment of inhibitory signaling molecules to BCR signalosomes.

Author contributions: M.K.S.-F. and W.S. designed research; M.K.S.-F., L.J.L., M.R.S., O.O.O., and S.P. performed research; S.P., X.Z., T.-H.T., and A.U. contributed new reagents/analytic tools; M.K.S.-F. and W.S. analyzed data; and M.K.S.-F. and W.S. wrote the paper.

The authors declare no conflict of interest.

This article is a PNAS Direct Submission. R.P. is a guest editor invited by the Editorial Board.

[1]To whom correspondence should be addressed. E-mail: wenxsong@umd.edu.

This article contains supporting information online at www.pnas.org/lookup/suppl/doi:10.1073/pnas.1321971111/-/DCSupplemental.

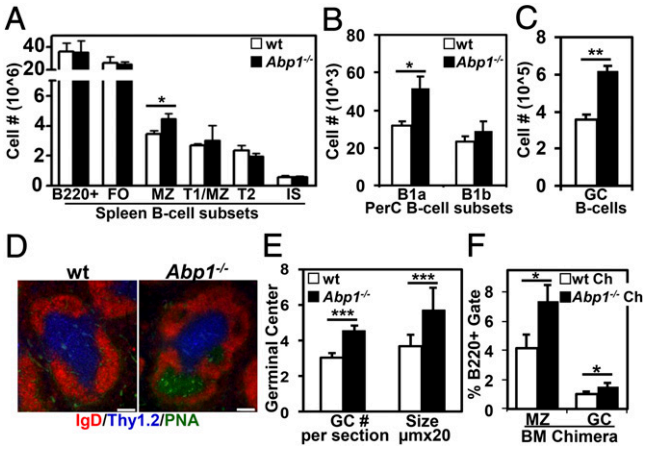

Fig. 1. B-cell–specific Abp1 deficiency is sufficient to increase the differentiation of MZ and spontaneous GC B cells. (*A–C*) Peripheral B-cell subsets in *Abp1*$^{-/-}$ and wt mice. Cells from spleens (*A*) and PerC (*B*) were labeled for surface markers of transitional 1 (T1), transitional 2 (T2), follicular (FO), marginal zone (MZ), isotype switched (IS) B cells or B1a and B1b B cells and were analyzed by flow cytometry. Shown are average numbers (+SD) of cells per spleen (*A*) ($n = 5$) or in the PerC (*B*) ($n = 4$). (*C*) Average numbers of GC B cells per spleen by flow cytometry (+SD; $n = 4$). (*D*) Immunofluorescent staining images of spleen sections from mice (6 mo old). (Scale bar, 100 µm.) $n = 12$ sections/4 wt or *Abp1*$^{-/-}$ mice. (*E*) Average numbers of PNA$^+$ GCs per spleen section and average length of GC (µm × 20) (+SD; $n = 12$ sections/4 wt or *Abp1*$^{-/-}$ mice). (*F*) Average percentages of MZ and GC B cells in B220$^+$ splenic B cells of wt-Ch and *Abp1*$^{-/-}$-Ch by flow cytometry (+SD; $n = 3$). $^*P < 0.05$; $^{**}P < 0.01$; $^{***}P < 0.001$.

internalization (20). However, how Abp1 contributes to BCR signaling remains unexplored.

This study demonstrates that Abp1 is a negative regulator of BCR signaling and B-cell activation. *Abp1*$^{-/-}$ B cells display greater levels of BCR signaling than wild-type (wt) B cells, which correlates with increased numbers of spontaneously formed GC B cells and autoAb production in *Abp1*$^{-/-}$ mice and bone marrow chimeric mice. Abp1 attenuates BCR signaling by promoting BCR microcluster coalescence and B-cell contraction and recruiting the inhibitory molecules SHIP-1 and HPK1 to BCR microclusters. Thus, our results reveal Abp1 as a novel mechanistic link between actin remodeling and negative signaling, exerting a B cell-intrinsic inhibition on B-cell activation.

Results

B-Cell–Specific Abp1 Deficiency Is Sufficient to Increase the Development of Marginal Zone and Germinal Center B Cells. Previous studies showed no significant defect in T-cell development in *Abp1*$^{-/-}$ mice (18), but whether Abp1 contributes to B-cell development has not been fully examined. The numbers and percentages of various B-cell subpopulations in the bone marrow, spleen, and peritoneal cavity (PerC) from *Abp1*$^{-/-}$ and age-matched wt mice were analyzed by flow cytometry (Fig. 1 and Fig. S1). *Abp1*$^{-/-}$ mice had normal percentages of all B-cell subsets in the bone marrow (Fig. S1 *A* and *B*). The numbers of splenic transitional 1 (T1) and 2 (T2), follicular, and isotype switched B cells were unaffected in *Abp1*$^{-/-}$ mice; however, the number of marginal zone (MZ) B cells was increased compared with wt mice (Fig. 1*A* and Fig. S1*C*). The number of B1a B cells in the PerC was also increased compared with wt mice (Fig. 1*B* and Fig. S1*D*). In addition, Abp1 expression levels in mature B cells of the spleen were much higher than those in pro- and pre-B cells (Fig. S1*E*), suggesting the defect observed in peripheral B-cell development in *Abp1*$^{-/-}$ mice may be related to differential expression of Abp1 in different B-cell subsets.

As mature B cells are activated in follicles to form GCs, we examined the number of GC B cells in the spleen of nonimmunized mice, using flow cytometry and immunohistochemistry. Nonimmunized *Abp1*$^{-/-}$ mice had significantly higher numbers of splenic GC B cells than wt mice (Fig. 1*C* and Fig. S1*F*). Consistent with this result, immunohistological examination showed increased numbers and larger sizes of PNA$^+$ GCs in *Abp1*$^{-/-}$ spleens compared with wt (Fig. 1 *D* and *E*). *Abp1*$^{-/-}$ mice also exhibit splenomegaly (Fig. S1*G*).

To examine whether the phenotype observed in *Abp1*$^{-/-}$ mice is B-cell intrinsic, we generated bone marrow chimeric mice (21). Lethally irradiated mice were transplanted with mixed bone marrow cells from B-cell null µMT and *Abp1*$^{-/-}$ or wt mice in an 80:20 ratio. Flow cytometry confirmed that only B cells lacked Abp1 expression in fully reconstituted *Abp1*$^{-/-}$ chimeric mice (*Abp1*$^{-/-}$-Ch; Figs. S2 and S3). Similar to *Abp1*$^{-/-}$ mice, *Abp1*$^{-/-}$-Ch mice displayed higher numbers of spontaneous GC and MZ B cells (Fig. 1*F*) in the spleen compared to those in wt chimeric mice (wt-Ch).

Taken together, these results suggest that Abp1 exerts a B-cell-intrinsic inhibition on the spontaneous development of GC B cells and differentiation of MZ and B1a B cells but is not involved in early B-cell maturation in the bone marrow.

Production of AutoAb, T-Independent Ab Responses and Total Ab Increase While T-Dependent High-Affinity Ab Responses Decrease in *Abp1*$^{-/-}$ Mice. Spontaneous GC formation has been described as a characteristic of autoimmune-susceptible mouse strains (22). To test this possibility, we evaluated autoAb production in

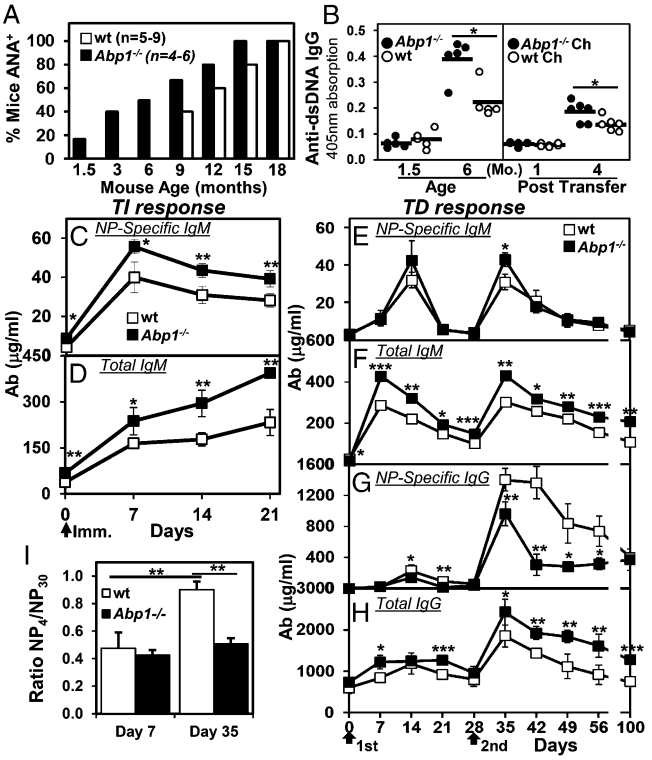

Fig. 2. Production of autoAb, T-independent Ab responses, and total Ab increases while T-dependent high-affinity Ab responses decrease in *Abp1*$^{-/-}$ mice. (*A*) Immunofluorescence microscopy analysis of antinuclear Ab in the serum of nonimmunized wt and *Abp1*$^{-/-}$ mice ($n = 4$~9) at different ages. (*B*) ELISA quantification of anti-dsDNA Ab in the serum of wt and *Abp1*$^{-/-}$ mice of 1.5 and 6 mo of age, and wt-Ch and *Abp1*$^{-/-}$-Ch mice at 1 and 4 mo posttransplant. Dots represent individual mice. (*C–H*) 6~8-wk-old mice ($n = 4$~5) were immunized with NP-Ficoll (*C* and *D*) or NP-KLH (*E–H*). NP-specific IgM (*C* and *E*), total IgM (*D* and *F*), NP-specific IgG (*G*), or total IgG (*H*) in the serum (µg/mL) determined by ELISA. (*I*) Relative affinity of NP-specific IgG in NP-KLH-immunized mice assessed as the concentration ratio of IgG bound to NP_4 versus NP_{30} by ELISA (+SD; $n = 4$~5). $^*P < 0.05$; $^{**}P > 0.01$; $^{***}P < 0.001$.

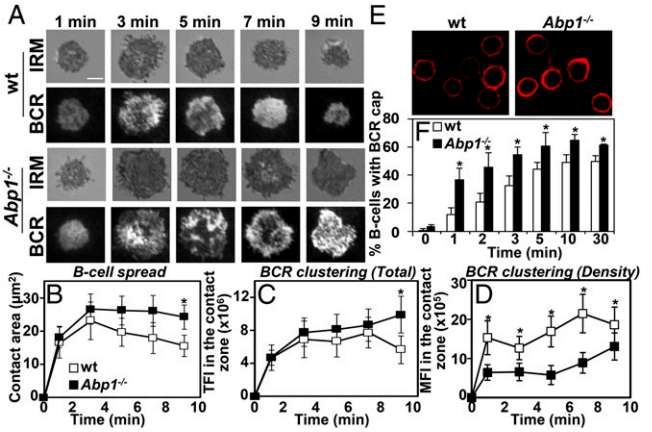

Fig. 3. Abp1 knockout augments B-cell spread and BCR clustering. (*A–D*) IRM and TIRF analysis of wt and *Abp1*$^{-/-}$ splenic B cells incubated with Fab'-anti-Ig-tethered lipid bilayers. Representative images. (Scale bar, 5 μm; $n = 3$) (*A*). Average contact area (*B*), TFI (*C*), and MFI (*D*) of labeled BCRs from >50 cells per time point ($n = 3$), quantified using Andor iQ software. (*E* and *F*) Confocal analysis of splenic B cells stained with AF546-mB-Fab'–anti-IgG+M and then streptavidin to activate. Representative images at 1 min (*E*) and average percentage (+SD) of cells showing polarized BCR caps (*F*) quantified from >100 cells per time point ($n = 3$; scale bar, 5 μm). *$P < 0.05$.

nonimmunized wt and *Abp1*$^{-/-}$ mice. Using an antinuclear Ab slide test (ANA), we found that *Abp1*$^{-/-}$ mice tested ANA-positive much earlier, with 50% positive by 6 mo of age compared with 0% of wt mice (Fig. 2*A*). Quantitative ELISA analysis showed that nonimmunized *Abp1*$^{-/-}$ mice had significantly higher anti-dsDNA Ab production than wt mice by 6 mo of age (Fig. 2*B*). Furthermore, *Abp1*$^{-/-}$-Ch mice also showed elevated levels of anti-dsDNA Ab compared with wt-Ch mice 4 mo after bone marrow transplant (Fig. 2*B*).

To examine whether increased MZ, B1a, and GC B cells in *Abp1*$^{-/-}$ mice affect Ab responses, we immunized mice with the T-independent Ag 4-hydroxy-3-nitrophenylacetyl (NP) conjugated to Ficoll once or the T-dependent Ag NP conjugated to Keyhole Limpet Hemocyanin (KLH) twice, 28 d apart, and quantified NP-specific and total IgM and/or IgG in the serum, using ELISA. In response to NP-Ficoll, *Abp1*$^{-/-}$ mice exhibited significant increases in both NP-specific (Fig. 2*C*) and total IgM (Fig. 2*D*) compared with wt mice. In response to NP-KLH, *Abp1*$^{-/-}$ mice showed slightly elevated Ag-specific IgM at day 35, but total IgM was significantly increased throughout the time course compared with wt mice (Fig. 2 *E* and *F*). Similar to a previous report (18), serum levels of Ag-specific IgG were decreased in *Abp1*$^{-/-}$ mice compared with wt mice (Fig. 2*G*). This decrease was especially dramatic after the boost, indicating that the secondary response is more severely affected by Abp1 deficiency. In contrast, the level of total IgG was significantly elevated in *Abp1*$^{-/-}$ mice during both primary and secondary Ab response (Fig. 2*H*). We further evaluated Ab affinity in NP-KLH immunized mice by determining the ratio of Ab binding to low-valent (NP_4) and high-valent (NP_{30}) Ag by ELISA. The ratio was significantly increased in wt mice but not in *Abp1*$^{-/-}$ mice after the boost (Fig. 2*I*). Thus, *Abp1*$^{-/-}$ mice display impaired affinity maturation and mount defective T-dependent Ab responses but elevated T-independent, nonspecific, and self-reactive Ab responses.

Abp1 Deficiency Augments B-Cell Spread and BCR Clustering. As the increased production of spontaneous GC B cells and autoAb is a B-cell–intrinsic effect, we further examined the effect of Abp1 deficiency on early events of BCR-mediated B-cell activation, including BCR clustering and B-cell morphological changes. We labeled and cross-linked surface BCRs using Alexa Fluor 546-labeled, monobiotinylated Fab' fragment of anti-mouse IgG+M Ab (AF546-mB-Fab'–anti-Ig) tethered to planar lipid bilayers (Fab'-anti-Ig-tethered lipid bilayers). Interference reflection microscopy (IRM) was used to analyze the area of the B-cell membrane that contacts the Fab'-anti-Ig-tethered surface (B-cell contact zone), which reflects B-cell spreading and contraction, as well as total internal reflection fluorescence microscopy (TIRF) to quantify relative amounts of BCRs clustered in the contact zone. We also analyzed BCR clustering in B cells stimulated with AF546-mB-Fab'–anti-IgG+M cross-linked by soluble streptavidin, using confocal microscopy. We found that the contact area of *Abp1*$^{-/-}$ B cells did not reduce after 3 min of activation, as did that of wt B cells, indicating an inhibition of cell contraction (Fig. 3 *A* and *B*). Total fluorescence intensity (TFI) of labeled BCRs in the contact zone of *Abp1*$^{-/-}$ B cells continuously increased over time compared with wt B cells which reached a plateau at 3 min and decreased by 9 min (Fig. 3*C*). However, the mean fluorescence intensity (MFI) of BCR staining in the contact zone of *Abp1*$^{-/-}$ B cells was lower than that of wt B cells (Fig. 3*D*). Labeled BCRs remained punctate throughout the contact zone of *Abp1*$^{-/-}$ B cells and did not coalesce into a central cluster by 7 min, as in wt B cells (Fig. 3*A*). In response to soluble BCR cross-linking, a significantly higher percentage of *Abp1*$^{-/-}$ B cells showed polarized BCR caps compared with wt B cells (Fig. 3 *E* and *F*). Together, these results indicate that *Abp1*$^{-/-}$ B cells sequester greater amounts of BCRs in the contact zone or polarized BCR caps on encountering Ag but are defective in the contraction and formation of BCR central clusters.

Abp1 Is Recruited to B-Cell Contact Zone upon BCR Activation. To understand the mechanism by which Abp1 contributes to BCR signaling, we examined the spatial relationship of Abp1 with BCRs at the cell surface. Upon incubation with Fab'-anti-Ig-tethered lipid bilayers, Abp1 was recruited to the B-cell contact zone (Fig. 4*A*). Although the contact zone area and size of BCR clusters changed over time, Abp1 predominantly accumulated at the outer edge of the contact zone and did not significantly colocalize with surface BCRs throughout the activation process (Fig. 4 *A* and *B*). Abp1 MFI rose over time, with a dramatic peak of recruitment at 7 min, concurrent with B-cell contraction but long after peak BCR TFI and maximal B-cell spreading (Figs. 3 *B* and *C* and 4*C*). These results indicate that Abp1 is specifically recruited to the periphery of the B-cell membrane, predominantly during B-cell contraction, in response to BCR activation.

BCR Signaling Is Enhanced in *Abp1*$^{-/-}$ B Cells. Increased numbers of spontaneous GC B cells, autoAb, and total Ab suggest augmented B-cell activation in *Abp1*$^{-/-}$ B cells. To investigate this possibility, we examined BCR-induced activation of proximal and distal signaling molecules in *Abp1*$^{-/-}$ B cells after BCR

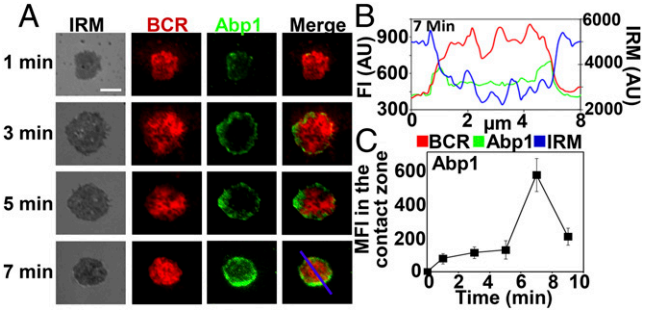

Fig. 4. BCR activation induces recruitment of Abp1 to the outer edge of the spreading B cell. (*A*) TIRF and IRM analysis of Abp1 in the contact zone of splenic B cells incubated with Fab'-anti-Ig-tethered lipid bilayers. Representative images ($n = 3$; scale bar, 5 μm). (*B*) Relative intensity of IRM and fluorescence intensity of BCRs and Abp1 across the blue line in cell at 7 min (*A*). (*C*) Average MFI of Abp1 (±SD) from >50 cells for each point quantified using Andor iQ ($n = 3$).

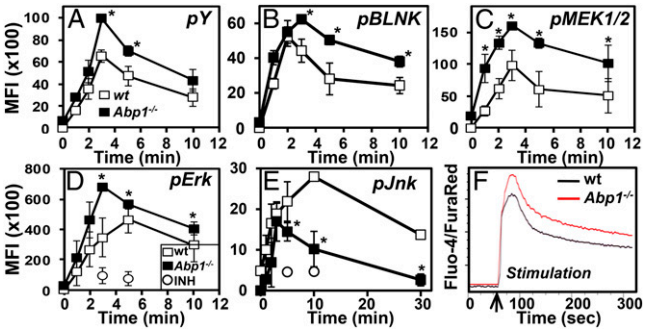

Fig. 5. BCR signaling is enhanced in $Abp1^{-/-}$ B cells. (*A–E*) Splenic B cells from wt and $Abp1^{-/-}$ mice were activated with F(ab')$_2$-goat anti-mouse IgG+M, fixed, permeabilized, labeled for phosphotyrosine (pY) (*A*), pBLNK (*B*), pMEK1/2 (*C*), pErk (*D*), and pJnk (*E*) and analyzed by flow cytometry (average MFI ± SD; $n = 3$). (*D* and *E*) Upstream Erk and Jnk inhibitor controls (INH) at indicated times. (*F*) Ca^{2+} flux in splenic B cells activated with F(ab')$_2$-goat anti-mouse IgG+M, using flow cytometry ($n = 3$). *$P < 0.05$.

cross-linking by flow cytometry. $Abp1^{-/-}$ B cells exhibited increased levels of tyrosine phosphorylation (Fig. 5*A*) and phosphorylated BLNK (pBLNK) (Fig. 5*B*). However, activation of MAP kinases was differentially affected. Phosphorylated mitogen-activated protein kinase kinase MEK1/2 (pMEK1/2) (Fig. 5*C*) and its downstream target Erk (pErk) (Fig. 5*D*) were significantly increased on BCR activation in $Abp1^{-/-}$ B cells compared with wt B cells. The levels of these phosphorylated proteins also took much longer to return to basal levels in the $Abp1^{-/-}$ B cells compared with wt B cells (Fig. 5 *A–D*). In contrast, phosphorylated Jnk (pJnk) was significantly reduced (Fig. 5*E*), whereas phosphorylated p38 (pp38) was unchanged in $Abp1^{-/-}$ B cells (Fig. S4). Treatment with Erk or Jnk inhibitors reduced the levels of pErk and pJnk to basal levels (Fig. 5 *D* and *E*), confirming staining specificity. Consistent with enhanced signaling, $Abp1^{-/-}$ B cells displayed higher Ca^{2+} flux than their wt counterparts (Fig. 5*F*). There was no significant difference in the expression levels of membrane IgM, BLNK, MEK1/2, Erk, and Jnk between resting $Abp1^{-/-}$ and wt B cells (Fig. S5 *A–E*). This result indicates that the enhanced signaling in $Abp1^{-/-}$ B cells is not a result of increased expression of BCRs or signaling molecules.

Abp1 Is Required for the Recruitment of HPK1 and SHIP-1 to the B-Cell Contact Zone. Enhanced signaling in $Abp1^{-/-}$ B cells suggests a negative regulatory role for Abp1 in BCR signaling. One possible mechanism by which Abp1 may negatively regulate signaling is by modulating inhibitory signaling molecules downstream of the BCR. To test this hypothesis, we examined the effects of Abp1 deficiency on the recruitment of two known inhibitory molecules, HPK1 and SHIP-1, to the B-cell contact zone using TIRF. Upon interaction with Fab'-anti-Ig-tethered lipid bilayers, the MFI of both HPK1 (Fig. 6 *A* and *B*) and phosphorylated SHIP-1 (pSHIP-1) (Fig. 6 *C* and *D*) in the contact zone of wt B cells increased over time, peaking by 7 min, and then reducing by 9 min. Although $Abp1^{-/-}$ B cells displayed the same trend of HPK1 recruitment, its MFI in the contact zone was significantly reduced throughout the time course. Similarly, the peak MFI of pSHIP in $Abp1^{-/-}$ B cells at 7 min was drastically reduced compared with wt B cells. However, Abp1 deficiency had no significant effect on the recruitment of phosphorylated spleen tyrosine kinase (pSyk) to BCR clusters (Fig. 6 *E* and *F*), as well as the expression levels of HPK1 and SHIP (Fig. S5 *F* and *G*). These results indicate that Abp1 is required for the recruitment and activation of the key inhibitory molecules HPK1 and SHIP-1 downstream of BCR stimulation.

Abp1 Regulates BCR-Induced Actin Reorganization. Increased B-cell spreading and BCR clustering at the surface of $Abp1^{-/-}$ B cells, which are actin-dependent events, suggest a role for Abp1 in BCR-induced actin remodeling. To investigate this hypothesis, we examined the effects of Abp1 deficiency on F-actin accumulation at the B-cell contact zone using TIRF. In wt B cells, F-actin MFI in the contact zone peaked at ∼3 min of incubation with Fab'-anti-Ig-tethered lipid bilayers, when B-cell spreading is maximal, and then reduced as B cells contracted (Fig. 7 *A* and *B*). In contrast, F-actin MFI in the contact zone of $Abp1^{-/-}$ B cells rose slowly, did not peak until ∼7 min, and remained at peak levels through 9 min. As levels of F-actin in resting B cells were not altered by Abp1 deficiency (Fig. S5*H*), our data suggest that Abp1 may primarily contribute to signal-induced actin remodeling, both early accumulation and later clearance of F-actin from the B-cell contact zone.

Abp1 has been shown to regulate actin dynamics by interacting with the actin nucleation promoting factor *N*-WASP in neurons (23). Our recent studies demonstrate that WASP plays a dominant role in actin assembly during B-cell spreading, but *N*-WASP has a unique role in actin clearance during B-cell contraction (14). To investigate whether Abp1 regulates actin remodeling via WASP and *N*-WASP, we analyzed the effect of Abp1 deficiency on the recruitment and phosphorylation of WASP (pWA) and *N*-WASP (pN-WA) by TIRF. In wt B cells, pWASP MFI peaked first at ∼5 min, followed by pN-WASP, which peaked at ∼7 min (Fig. 7 *C–F*) (14). In $Abp1^{-/-}$ B cells, pWASP MFI increased with the same kinetics and to similar levels as wt B cells but reduced more slowly after reaching maximal levels compared with wt (Fig. 7 *C* and *D*). In contrast, pN-WASP MFI in the contact zone of $Abp1^{-/-}$ B cells was significantly lower than wt B cells (Fig. 7 *E* and *F*). Flow cytometry analysis further confirmed reduced levels of pN-WASP in $Abp1^{-/-}$ B cells (Fig. S6). However, Abp1 deficiency has no significant effect on basal expression levels of WASP and *N*-WASP (Fig. S5 *I* and *J*). These results suggest that Abp1 regulates BCR-induced actin remodeling by suppressing WASP activation, which induces F-actin accumulation and B-cell spreading, and by enhancing *N*-WASP activation, which triggers actin clearance and B-cell contraction.

Discussion

Abp1, an actin-binding adaptor protein expressed widely from yeast to mammalian cells, has been implicated in a multitude of cellular functions, including endocytosis (19, 20, 24, 25), synaptic vesicle recycling (25), phagocytosis (26), cell migration (27, 28), and T-cell activation (18, 19). This study reveals a novel function for Abp1, attenuation of BCR signaling, which contributes to the regulation of peripheral B-cell differentiation and Ab responses.

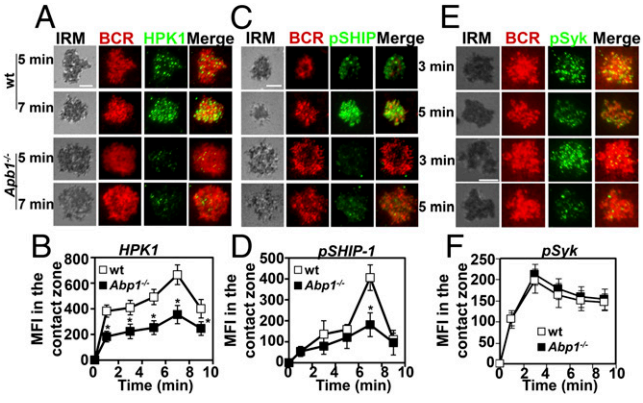

Fig. 6. Abp1 is required for recruitment of the inhibitory signaling molecules, HPK1 and SHIP-1, but not pSyk to the B-cell contact zone. TIRF analysis of HPK1 (*A* and *B*), phosphorylated SHIP-1 (pSHIP-1) (*C* and *D*) and Syk (pSyk) (*E* and *F*) in the contact zone of wt and $Abp1^{-/-}$ B cells incubated with Fab'-anti-Ig-tethered lipid bilayers. Shown are representative images and MFI (±SD) in the contact zone (50 cells per time point; $n = 3$; scale bar, 5 μm). *$P < 0.01$.

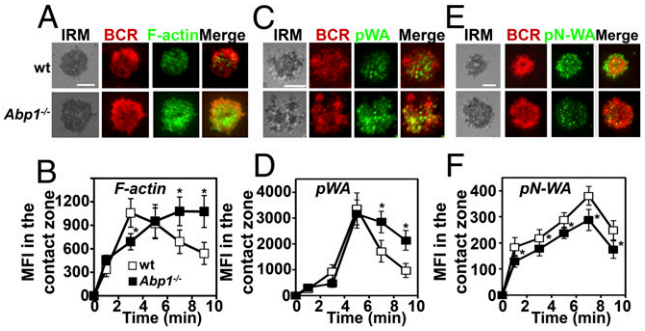

Fig. 7. Abp1 regulates actin remodeling by modulating activation of the actin nucleation promoting factors, WASP and *N*-WASP. (*A–F*) Splenic B cells from wt and *Abp1*$^{-/-}$ mice were activated with Fab′-anti-Ig-tethered lipid bilayers, fixed, permeabilized, and stained with AF488 phalloidin for F-actin (*A*), p-WASP (pWA) (*C*), or pN-WASP (pN-WA) (*E*). Representative images at 7 min ($n = 3$; Scale bar, 5 μm). The MFI (± SD) of F-actin (*B*), p-WASP (pWA) (*D*), and pN-WASP (pN-WA) (*F*) in the contact zone quantified in >50 cells per time point ($n = 3$). *$P < 0.05$.

Abp1 exerts a B-cell intrinsic inhibition both on spontaneous activation and differentiation of mature follicular and self-reactive B cells into GC B cells and Ab-secreting cells and on the generation of MZ and B1a B cells. Abp1 is required for B-cell affinity maturation and mounting effective T-dependent Ab responses. In addition to its role in BCR uptake of Ag for processing (20), Abp1 contributes to BCR signal attenuation by promoting B-cell contraction and BCR microcluster coalescence, as well as by recruitment of the inhibitory signaling molecules SHIP-1 and HPK1 to BCR microsignalosomes.

This study shows that the effects of Abp1 deficiency on the differentiation of MZ B cells and spontaneous GC B cells are B-cell intrinsic. The increased numbers of MZ, B1a, and GC B cells provide an explanation for the enhanced T-independent response and elevated autoAb levels in *Abp1*$^{-/-}$ mice. As expression levels of the BCR and signaling molecules are not altered in *Abp1*$^{-/-}$ B cells, our results support the notion that Abp1-mediated down-regulation of BCR signaling directly influences the differentiation of these peripheral B-cell subsets. These data also suggest that Abp1 is potentially involved in suppressing Ag-independent signals required for the differentiation of GC, MZ, and B1a B cells. Actin dynamics are known to regulate tonic BCR signaling via modulating BCR–BCR and BCR–CD19 interactions (29). Thus, it is possible that Abp1 regulates tonic signaling in resting B cells by modulating actin dynamics and receptor interactions. Additional research is required to address these questions.

Failure of *Abp1*$^{-/-}$ mice to generate high-affinity Ab while simultaneously producing high levels of nonspecific IgG during T-dependent Ab responses indicates defective affinity maturation. In GCs, B cells with higher-affinity BCRs are selected to survive and differentiate because of a greater ability to signal and capture/present Ag to T cells than low-affinity B cells (30). Enhanced/prolonged BCR signaling in *Abp1*$^{-/-}$ B cells may interfere with affinity-dependent signal regulation. Reductions in Ag uptake and presentation (20) likely ablate the ability of *Abp1*$^{-/-}$ B cells to acquire T-cell help. Impairment in the activation of *Abp1*$^{-/-}$ T cells may further exacerbate the affinity maturation defect observed in *Abp1*$^{-/-}$ mice. The affinity maturation defect provides another possible explanation for increased levels of autoAb in *Abp1*$^{-/-}$ mice, as Ag-specific B cells are not preferentially selected from B-cell pools that also contain autoreactive B cells.

The negative regulatory function of Abp1 in BCR signaling demonstrated here is in contrast to its positive role in T-cell receptor (TCR) activation (18). Although T-cell development is largely unchanged in *Abp1*$^{-/-}$ mice, TCR-induced phosphorylation of the linker for activation of T cells LAT and PLCγ1, and activation of the MAP kinases JNK and p38, are partially defective, and T-cell proliferation and cytokine production are reduced (18). Similar to T cells (18), Abp1 deficiency does not have a significant effect on early B-cell development; however, BCR signaling is enhanced in *Abp1*$^{-/-}$ B cells upon in vitro stimulation, exhibiting higher levels of tyrosine and BLNK phosphorylation. Although JNK phosphorylation is decreased, similar to *Abp1*$^{-/-}$ T cells, *Abp1*$^{-/-}$ B cells display faster kinetics and higher levels of ERK phosphorylation than wt B cells. The *Abp1*$^{-/-}$ mice used here were generated by the laboratory that reported the T-cell study (18), and therefore, opposing functions in T and B cells cannot be attributed to differences in the mouse model. Although the molecular mechanisms underlying differential regulation of BCR and TCR signaling remain elusive, our results demonstrate cell type-specific functions for Abp1 in signal regulation.

This and previous studies (16, 18, 20, 23, 24) suggest three mechanisms by which Abp1 may promote signal attenuation, including modulating actin dynamics and actin-dependent early BCR activation events, the recruitment of inhibitory signaling molecules, and BCR internalization. We previously demonstrated that although BCR clustering initiates signaling, the subsequent coalescence of BCR microclusters into central clusters attenuates signaling (8, 9, 14). Formation of BCR clusters depends on actin remodeling, which controls lateral movement of BCRs and mediates B-cell morphological changes. B-cell spreading amplifies BCR clustering, and B-cell contraction drives microcluster coalescence (8, 9, 13). This study shows that Abp1 is not required for BCR microcluster formation and B-cell spreading, but instead facilitates B-cell contraction and BCR microcluster coalescence. Abp1-mediated signal attenuation may be attributed to its role in actin remodeling, where Abp1 plays a more prominent role in actin clearance rather than actin accumulation in the B-cell contact zone. In support of this hypothesis, failure to clear F-actin in the contact zone of *N-WASP*$^{-/-}$ B cells has been linked to enhanced and prolonged BCR signaling (14).

How Abp1 regulates BCR-induced actin remodeling is not fully understood. Although yeast Abp1 directly activates Arp2/3 (31), mammalian Abp1 may regulate actin polymerization indirectly by interactions with *N*-WASP, as reported in neurons (23). Unlike neurons, immune cells express both *N*-WASP and its hematopoietic homolog WASP, and the two have distinct functions in B cells. WASP activates actin assembly and B-cell spreading, whereas *N*-WASP promotes F-actin clearance and B-cell contraction. Furthermore, these two negatively regulate one another (14). We show here that levels of active WASP and *N*-WASP are increased and decreased in *Abp1*$^{-/-}$ B cells, respectively. This suggests that Abp1 preferentially promotes *N*-WASP activation, which suppresses WASP activation. Similar recruitment kinetics for *N*-WASP (14) and Abp1 to the B-cell contact zone and similar phenotypes observed in *Abp1*$^{-/-}$ and *N-WASP*$^{-/-}$ mice further support a functional relationship between the two and the notion that Abp1 modifies actin remodeling by regulating *N*-WASP.

Abp1 is responsible for bringing HPK1 to the immunological synapse of T cells (19). We confirm here that Abp1 has a similar role in B cells. Activated HPK1 is known to phosphorylate BLNK, leading to ubiquitination and down-regulation of BLNK (6). Although we did not directly examine HPK1 activation here, elevated levels of phosphorylated BLNK and ERK, and Ca^{2+} flux in *Abp1*$^{-/-}$ B cells suggest that Abp1 is involved in HPK1 activation. Surprisingly, BCR-induced activation and recruitment of SHIP-1 requires Abp1. SHIP-1 is known to inhibit signaling downstream of the BCR and B-cell proliferative responses critical for affinity maturation of B cells (5, 7). *SHIP-1*$^{-/-}$ B cells exhibit delayed BCR microcluster coalescence and B-cell contraction (8). *Abp1*$^{-/-}$ mice and B cells share many of the phenotypes observed in *SHIP-1*$^{-/-}$ and *HPK1*$^{-/-}$ mice and B cells, suggesting that recruitment of SHIP-1 and HPK1 to surface BCRs is the primary mechanism underlying Abp1-mediated negative regulation of BCR signaling and B-cell activation. The question remains, however, how Abp1 brings SHIP-1 to BCR signalosomes.

Abp1 can promote signal attenuation by moderating BCR internalization. It has been shown that inhibition of BCR endocytosis

by perturbing actin and *N-WASP*$^{-/-}$ enhances signaling (9, 14, 32). Abp1 facilitates BCR internalization by bridging actin and dynamin 2 at constricted necks of endocytosing vesicles (20, 24, 26). Although Abp1 likely uses multiple mechanisms in downregulating BCR signaling, it should be noted that these mechanisms are likely interrelated: Abp1-modulated actin remodeling may be important for recruitment of HPK1 and SHIP-1, and recruited inhibitory signaling molecules can regulate actin remodeling and actin-mediated cellular events.

This study further demonstrates the importance of actin in negative regulation of B-cell activation and identifies Abp1 as a missing link between actin and signal attenuation mechanisms, which expands our understanding of the molecular mechanisms underlying negative regulation of B-cell activation.

Materials and Methods

Mice and Cell Culture. Abp1 knockout mice (*Abp1*$^{-/-}$) were previously described (18). All other mice were purchased from Jackson Laboratory. Splenic B cells were enriched, and bone marrow and peritoneal cells were flushed from femurs and PerCs, respectively. All animal work was approved by the Institutional Animal Care and Use Committee of the University of Maryland.

Flow Cytometry. Cells were preincubated with Fcγ receptor block (BD Bioscience) and stained with Abs specific for different surface markers at 4 °C. To stain intracellular molecules, cells were activated with F(ab')$_2$-goat anti-mouse IgG+M (Jackson ImmunoResearch), fixed, permeabilized, and labeled with Abs specific for signaling molecules or Abp1 (20). Cells were analyzed using a FACSCanto flow cytometer (BD Biosciences).

Immunohistochemistry. Spleens embedded in optimum cutting temperature compound OCT (Sakura Finetek) were sectioned using a cryostat. Samples were fixed, stained with fluorescently conjugated Abs, and imaged using a Zeiss LSM710 confocal microscope.

Serological Analysis and Immunizations. Antinuclear Abs were detected using ANA (HEp-2) slides (MBL-Bion). Levels of anti-dsDNA Abs were quantified by ELISA (21). Mice were immunized (intraperitoneally) with (4-hydroxy-3-nitrophenyl)acetyl conjugated to Ficoll or keyhole limpet hemocyanin (NP-Ficoll or NP-KLH; Biosearch Technologies) in PBS or Sigma Adjuvant (Sigma-Aldrich), respectively, and boosted on day 28 (NP-KLH only). Levels of NP-specific and total IgM and IgG Abs were determined by ELISA. Relative affinity was assessed as the concentration ratio of IgG bound to NP_4- versus NP_{30}-BSA by ELISA.

Bone Marrow Chimeric Mice. Lethally irradiated (1,000 cGy) wt C57BL/6 (CD45.1) mice were transplanted with BM cells (1×10^7) from *Abp1*$^{-/-}$ or wt mice mixed at a 20:80 ratio with μMT BM (CD45.2) (21). Plasma cells were depleted from donor BM by incubation with biotin-anti-CD138 (BD Biosciences), followed by EasySep Streptavidin RapidSpheres and an EasySep Magnet (Stem Cell Technologies).

Total Internal Reflection Fluorescence Microscopy. Alexa Fluor 546-conjugated, monobiotinylated Fab' fragment of anti-mouse antibody (AF546-mB-Fab'-anti-IgG+M) tethered to planar lipid bilayers was generated to stimulate B cells, as previously described (33). Images were acquired using a Nikon laser TIRF system (Nikon TE2000-PFS, 60× TIRF objective). For intracellular molecules, B cells were fixed, permeabilized, and stained with specific Abs or AF488-phalloidin for F-actin. Total or mean fluorescence intensity was determined using Andor iQ software (Andor Technology).

Confocal Microscopic Analysis. Splenic B cells were stained with AF546-mB-Fab'–anti-IgG+M for surface BCRs and streptavidin to activate and were analyzed with a confocal microscope.

Calcium Analysis. Calcium flux was analyzed with Fluo4 AM and Fura Red (Invitrogen), using manufacturer's protocols and a flow cytometer (BD Biosciences).

For detailed materials and methods, see *SI Materials and Methods*.

ACKNOWLEDGMENTS. We thank Dr. Mark Jenkin (US Department of Agriculture), Amy Beaven (Imaging core), and Kenneth Class (Flow Cytometry core) for technical assistance. This work was supported by grants from the National Institutes of Health (AI059617) and from Maryland Stem Cell Research Fund (to W.S.).

1. Harwood NE, Batista FD (2010) Early events in B cell activation. *Annu Rev Immunol* 28: 185–210.
2. Dal Porto JM, et al. (2004) B cell antigen receptor signaling 101. *Mol Immunol* 41(6-7): 599–613.
3. Dykstra M, Cherukuri A, Sohn HW, Tzeng SJ, Pierce SK (2003) Location is everything: Lipid rafts and immune cell signaling. *Annu Rev Immunol* 21:457–481.
4. Youinou P, et al. (2006) B lymphocytes on the front line of autoimmunity. *Autoimmun Rev* 5(3):215–221.
5. Leung WH, Tarasenko T, Bolland S (2009) Differential roles for the inositol phosphatase SHIP in the regulation of macrophages and lymphocytes. *Immunol Res* 43(1-3):243–251.
6. Wang X, et al. (2012) Down-regulation of B cell receptor signaling by hematopoietic progenitor kinase 1 (HPK1)-mediated phosphorylation and ubiquitination of activated B cell linker protein (BLNK). *J Biol Chem* 287(14):11037–11048.
7. Leung WH, et al. (2013) Aberrant antibody affinity selection in SHIP-deficient B cells. *Eur J Immunol* 43(2):371–381.
8. Liu C, et al. (2011) A balance of Bruton's tyrosine kinase and SHIP activation regulates B cell receptor cluster formation by controlling actin remodeling. *J Immunol* 187(1):230–239.
9. Liu C, et al. (2012) Actin reorganization is required for the formation of polarized B cell receptor signalosomes in response to both soluble and membrane-associated antigens. *J Immunol* 188(7):3237–3246.
10. Treanor B, et al. (2010) The membrane skeleton controls diffusion dynamics and signaling through the B cell receptor. *Immunity* 32(2):187–199.
11. Freeman SA, et al. (2011) Cofilin-mediated F-actin severing is regulated by the Rap GTPase and controls the cytoskeletal dynamics that drive lymphocyte spreading and BCR microcluster formation. *J Immunol* 187(11):5887–5900.
12. Harwood NE, Batista FD (2011) The cytoskeleton coordinates the early events of B-cell activation. *Cold Spring Harb Perspect Biol*, 10.1101/cshperspect.a002360.
13. Fleire SJ, et al. (2006) B cell ligand discrimination through a spreading and contraction response. *Science* 312(5774):738–741.
14. Liu C, et al. (2013) N-wasp is essential for the negative regulation of B cell receptor signaling. *PLoS Biol* 11(11):e1001704.
15. Larbolette O, Wollscheid B, Schweikert J, Nielsen PJ, Wienands J (1999) SH3P7 is a cytoskeleton adapter protein and is coupled to signal transduction from lymphocyte antigen receptors. *Mol Cell Biol* 19(2):1539–1546.
16. Ensenat D, et al. (1999) A novel src homology 3 domain-containing adaptor protein, HIP-55, that interacts with hematopoietic progenitor kinase 1. *J Biol Chem* 274(48): 33945–33950.
17. Kessels MM, Engqvist-Goldstein AE, Drubin DG (2000) Association of mouse actin-binding protein 1 (mAbp1/SH3P7), an Src kinase target, with dynamic regions of the cortical actin cytoskeleton in response to Rac1 activation. *Mol Biol Cell* 11(1):393–412.
18. Han J, et al. (2005) HIP-55 is important for T-cell proliferation, cytokine production, and immune responses. *Mol Cell Biol* 25(16):6869–6878.
19. Le Bras S, et al. (2004) Recruitment of the actin-binding protein HIP-55 to the immunological synapse regulates T cell receptor signaling and endocytosis. *J Biol Chem* 279(15):15550–15560.
20. Onabajo OO, et al. (2008) Actin-binding protein 1 regulates B cell receptor-mediated antigen processing and presentation in response to B cell receptor activation. *J Immunol* 180(10):6685–6695.
21. Becker-Herman S, et al. (2011) WASp-deficient B cells play a critical, cell-intrinsic role in triggering autoimmunity. *J Exp Med* 208(10):2033–2042.
22. Luzina IG, et al. (2001) Spontaneous formation of germinal centers in autoimmune mice. *J Leukoc Biol* 70(4):578–584.
23. Pinyol R, Haeckel A, Ritter A, Qualmann B, Kessels MM (2007) Regulation of N-WASP and the Arp2/3 complex by Abp1 controls neuronal morphology. *PLoS ONE* 2(5):e400.
24. Kessels MM, Engqvist-Goldstein AE, Drubin DG, Qualmann B (2001) Mammalian Abp1, a signal-responsive F-actin-binding protein, links the actin cytoskeleton to endocytosis via the GTPase dynamin. *J Cell Biol* 153(2):351–366.
25. Connert S, et al. (2006) SH3P7/mAbp1 deficiency leads to tissue and behavioral abnormalities and impaired vesicle transport. *EMBO J* 25(8):1611–1622.
26. Gopaldass N, et al. (2012) Dynamin A, Myosin IB and Abp1 couple phagosome maturation to F-actin binding. *Traffic* 13(1):120–130.
27. Cortesio CL, Perrin BJ, Bennin DA, Huttenlocher A (2010) Actin-binding protein-1 interacts with WASp-interacting protein to regulate growth factor-induced dorsal ruffle formation. *Mol Biol Cell* 21(1):186–197.
28. Hepper I, et al. (2012) The mammalian actin-binding protein 1 is critical for spreading and intraluminal crawling of neutrophils under flow conditions. *J Immunol* 188(9): 4590–4601.
29. Mattila PK, et al. (2013) The actin and tetraspanin networks organize receptor nanoclusters to regulate B cell receptor-mediated signaling. *Immunity* 38(3):461–474.
30. Klein U, Dalla-Favera R (2008) Germinal centres: Role in B-cell physiology and malignancy. *Nat Rev Immunol* 8(1):22–33.
31. Goode BL, Rodal AA, Barnes G, Drubin DG (2001) Activation of the Arp2/3 complex by the actin filament binding protein Abp1p. *J Cell Biol* 153(3):627–634.
32. Hao S, August A (2005) Actin depolymerization transduces the strength of B-cell receptor stimulation. *Mol Biol Cell* 16(5):2275–2284.
33. Sohn HW, Tolar P, Pierce SK (2008) Membrane heterogeneities in the formation of B cell receptor-Lyn kinase microclusters and the immune synapse. *J Cell Biol* 182(2): 367–379.